Sensitivity Analysis of Digital Flight Control Systems Using Singular-Value Concepts

James D. Paduano* and David R. Downing†
University of Kansas Flight Research Laboratory, Lawrence, Kansas

A recently developed sensitivity analysis technique for linear control systems, which is based on the gradients of the return-difference-matrix singular values, is improved by introducing system scaling, and extended to include digital systems. System scaling is used to improve the reliability of the singular values as measures of relative stability. Digital systems are included in the analysis through the derivation of new equations for the matrix singular-value gradients. An example of the applicability of the method to high-order, digital, multiloop systems is presented using the X-29A lateral-directional control laws. Results for the X-29A are discussed, as well as the range of validity of these results.

Nomenclature

$\bar{A},\bar{B}$ = augmented system state-space dynamic matrices
A_c,B_c = continuous system state-space dynamic matrices
A_d,B_d = digital system state-space dynamic matrices
$\bar{C}$ = feedback matrix
C_1,C_2 = interconnection matrices
D = real diagonal scaling matrix
$G(s)$ = system transfer function matrix
H = altitude
H_c = continuous system output matrix
H_d = digital system output matrix
j = imaginary term $j=\sqrt{-1}$
$K(s)$ = controller transfer function matrix
L,L_i,L_o = disturbance matrices
M = Mach number
m = dimension of the control input vector $\boldsymbol{u}$
n = dimension of the state vector $\boldsymbol{x}$
p = any plant or control system parameter
$\boldsymbol{u}$ = control input vector
$\boldsymbol{x}$ = system state vector
$\boldsymbol{y}$ = system output vector
ϕ = transition matrix
ψ = integral of the transition matrix
σ = singular value, $\sigma_n=\sqrt{\lambda_n(A^*A)}$
$\underline{\sigma},\bar{\sigma}$ = minimum, maximum σ, respectively
σ_{ma} = minimum-allowable singular value
ω = frequency

Introduction

THE performance of a flight control system design is strongly affected by the accuracy of the model of the open-loop vehicle used during the design process. To ensure acceptable performance of the design on the real vehicle, the designer can either attempt to build insensitivity to model errors into the design (robust control) or require additional wind-tunnel or flight testing to assure the model's fidelity. Much work has been done in the area of robust control, and many techniques exist for assuring the insensitivity of the control system to variations in the model. Fewer techniques exist, however, for determining how additional wind-tunnel or flight testing should be conducted if it is deemed necessary. References 1 and 2 present such a technique: a sensitivity analysis that determines the specific model parameters that are most important to the stable operation of a continuous control system. The procedure is based on the singular values of the return difference matrix, and the gradients of these singular values with respect to system and controller parameters. In Refs. 1 and 2, singular-value gradients were demonstrated to be a viable way to determine which parameters, of the many that describe a control system, most strongly effect that system's relative stability.

This paper presents the extension of this analysis to digital systems, and attempts to improve the accuracy of the singular-value plot (σ-plot) as a measure of system relative stability. These extensions, with a few other modifications to the analysis, allow complex, high-order, digital systems to be analyzed. This paper will begin by discussing real diagonal scaling as a partial solution to the problem of the overconservative nature of singular values. It will then give a brief review of the technique introduced in Ref. 1, followed by a derivation of the singular-value gradients (σ-gradients) for digital systems. Next, the technique is applied to the linear model of the X-29A Advanced Technology Demonstrator; σ-plot results are given and the sensitivity analysis technique is demonstrated. The linearity of singular-value plots is then investigated to determine the range of usefulness of predictions that are based on σ-gradients.

Singular Value as a Measure of Relative Stability

Consider the control system in Fig. 1, where G is the transfer function matrix of the plant, K is the transfer function matrix of the controller, and L_i and L_o are perturbation matrices. It is well known [1-5] that if this system is stable when unperturbed (i.e., $L_o=L_i=I$), then a sufficient but not necessary condition for the system to remain stable is

$$L_o = I \tag{1a}$$

and

$$\bar{\sigma}(L_i^{-1}-I) < \underline{\sigma}[I+K(j\omega)G(j\omega)] \tag{1b}$$

Thus, $\underline{\sigma}(I+KG)$, the minimum singular value of the input node return difference matrix, is the basic robustness measure used by Refs. 1, 2, and 5-8. Since $\underline{\sigma}(I+KG)$ characterizes the

Received June 16, 1986; presented as Paper 86-2084 at the AIAA Guidance, Navigation and Control Conference, Williamsburg, VA, Aug. 18-20, 1986; revision received Dec. 15, 1987.

*Graduate Research Assistant. Member AIAA.
†Professor, Aerospace Engineering. Associate Fellow AIAA.

maximum allowable unstructured uncertainty L_i, it is conservative for any L_i that has a known structure, such as the commonly used gain-phase perturbation form

$$L_i = \text{diag}[k_1 e^{j\phi_1} \quad k_2 e^{j\phi_2} \ldots] \tag{2}$$

which yields boundaries for independent changes in gain and/or phase in each of the control loops.[3-6] These boundaries are useful because they are expressed in well-understood terms. Unfortunately, $\underline{\sigma}(I + KG)$ can yield very conservative boundaries for diagonal perturbations, because it also bounds crossfeed perturbations. This conservatism can be mitigated by scaling the system to maximize the singular values. Simple algorithms are available[9] to compute a real diagonal matrix D that maximizes the expression

$$\min_\omega \underline{\sigma}(I + D[K(j\omega)G(j\omega)]D^{-1}) \tag{3}$$

A real diagonal D represents a simple "change of units" that minimizes the effect of sensitivity to crossfeed perturbations. Thus, the conservatism of multiloop gain and phase margin predictions is minimized in general, and actually eliminated for cases where KG is of dimension 3×3 or less.[10]

A complementary form of the robustness problem is to let $L_i = I$ and use L_o to represent all unpredicted plant dynamics, including unmodeled crossfeeds or couplings in the plant. Crossfeed perturbations within the system are modeled by multiplying the output vector of the plant by an L_o, which has nonzero off-diagonal elements. This L_o feeds each output across to the other output channels after multiplying it by some gain and phase. The allowable sizes of the gain and phase perturbations in the crossfeed channels, as well as those along the diagonal of L_o, are determined by the size of $(I + GK)$, which is the output node return difference matrix. The relationship between $(I + GK)$ and L_o is analogous to that in Eq. (1); if the unperturbed system is stable, it will remain stable if

$$L_i = I \tag{4a}$$

and

$$\bar{\sigma}(L_o^{-1} - I) < \underline{\sigma}(I + GK) \tag{4b}$$

Along the diagonal of L_o, the multiplication factors described above make sense: they correspond to gain and phase changes. But off-diagonal elements of L_o are multiplication factors between channels, which may have different units. Thus, the "sizes" of the allowable multiplication factors depend on the relative units of the channels between which the crossfeeds occur. This dependence on the units of the output vector makes $\underline{\sigma}(I + GK)$ an unreliable measure of robustness, even for the unstructured uncertainties that one experiences at the plant output.

One possible approach to this problem is to "normalize" the relative units of the output vector, so that the off-diagonal elements of L_o again take on the interpretation of gain and phase margins. Normalization can be achieved by scaling the system so that during the normal operation of the plant, the elements of the output vector vary in magnitude between zero and one. Thus, allowable multiplication factors between channels have the same interpretation as those along the diagonal. Extra crossfeed "weighting" can be given to a channel by scaling it so that its magnitude is larger. This scaling concept can be implemented using simple, easily determined real diagonal matrices at the output of the plant and the input to the controller. The stability guarantee of Eqs. (4) applies, unfortunately, only to the scaled form of the control system,[3] but if the scaling chosen represents the real system's crossfeed behavior, this is not a problem. The goal of this type of scaling is not to provide stability guarantees or extremely accurate robustness quantification, but to provide a useful starting point for the sensitivity analysis, whose results are not particularly sensitive to small shifts in the $\underline{\sigma}$-plot.

The robustness problem has received considerable attention in recent years. Measures similar to singular values, but with improved properties, are available, e.g., Ref. 10. These alternate robustness measures will not be pursued in this paper because their gradients have not yet been studied. The gradients of singular values, on the other hand, are easy to compute. These gradients form the essential framework for the sensitivity analysis procedure introduced in Ref. 1 and extended in this paper. Therefore, singular values, scaled to improve their characteristics, are used as the measure of robustness and relative stability.

Singular-Value Gradients

The technique described in Ref. 1 uses the control system description

$$\dot{x} = \bar{A}x + \bar{B}u \tag{5}$$

$$u = -\bar{C}x \tag{6}$$

where x has n states and u has m controls. It then describes the equations that allow one to compute the gradient of the singular values

$$[\partial\sigma(I + KG)/\partial p](j\omega) \tag{7}$$

where p is any element of the $\bar{A}$, $\bar{B}$, or $\bar{C}$ matrix. These gradients, when normalized to take out the sizes of the elements themselves, can be plotted as functions of ω and compared to one another to determine which parameters are important to a control system's relative stability. By identifying the important parameters in the model of the control system, this sensitivity analysis can give the designer valuable information about whether the model is adequate and, if it is not, where it needs improvement.

A simple modification to the analysis described above is necessary to allow one to compute gradients with respect to parameters that do not appear explicitly as control system matrix elements. Computing such gradients is of interest because control system parameters such as loop gains and filter coefficients often affect many elements rather than a single element of $\bar{A}$, $\bar{B}$, or $\bar{C}$. Fortunately, a simple partial-derivative expansion can be used to analyze this kind of parameter. To this end, let p be any parameter in the control system. The

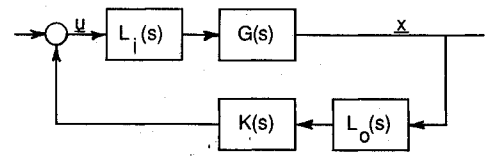

Fig. 1 Typical control system with disturbances at the input and output of the plant.

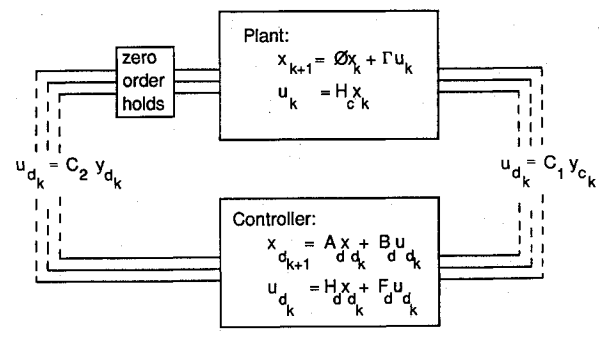

Fig. 2 Single-rate digital control system description.

gradient with respect to p can be computed as

$$\frac{\partial\sigma}{\partial p}=\sum_{i=1}^{n}\sum_{j=1}^{n}\frac{\partial\sigma}{\partial a_{ij}}\frac{\partial a_{ij}}{\partial p}+\sum_{i=1}^{n}\sum_{j=1}^{m}\frac{\partial\sigma}{\partial b_{ij}}\frac{\partial b_{ij}}{\partial p}+\sum_{i=1}^{m}\sum_{j=1}^{n}\frac{\partial\sigma}{\partial c_{ij}}\frac{\partial c_{ij}}{\partial p} \tag{8}$$

where $\partial a_{ij}/\partial p$, $\partial b_{ij}/\partial p$, and $\partial c_{ij}/\partial p$ represent the effects that a change in p would have on the control system matrix elements. Equation (8) is useful not only for control system parameters that affect many matrix elements, but also for simultaneous changes in plant parameters. In others words, if certain parameters are known to change simultaneously, a linear combination of these parameters can be introduced as a new parameter of study, using Eq. (8).

To extend this analysis to include digital systems, new formulas for the singular-value gradients are required. A single-rate digital control system can be represented with the following equations (see Fig. 2):

Plant:

$$\dot{x}_c = A_c x_c + B_c u_c \tag{9}$$

$$y_c = H_c x_c \tag{10}$$

Discretized plant:

$$x_{c_{k+1}} = \phi x_{c_k} + \psi B_c u_{c_k} \tag{11}$$

$$y_{c_k} = H_c x_{c_k} \tag{12}$$

where

$$\phi = I + A_c T + \frac{A_c^2 T^2}{2!} + \frac{A_c^3 T^3}{3!} + \cdots$$

and

$$\psi = \int_0^T \phi(\tau)\,d\tau$$

Controller:

$$x_{d_{k+1}} = A_d x_{d_k} + B_d u_{d_k} \tag{13}$$

$$y_{d_k} = H_d x_{d_k} + F_d u_{d_k} \tag{14}$$

Interconnections:

$$u_{d_k} = C_1 y_{c_k} \tag{15}$$

$$u_k = C_2 y_{d_k} \tag{16}$$

These equations can be coupled into a single system of the form

$$x_{k+1} = \bar{A} x_k + \bar{B} u_k \tag{17}$$

$$u_k = -\bar{C} x_k \tag{18}$$

where $\bar{A}$, $\bar{B}$, and $\bar{C}$ can be formulated to represent either the case where the disturbance matrix is placed at the plant input L_i, or the case where the disturbance matrix is placed at the plant output L_o. The scaling matrix D can also be imbedded in this formulation without loss of generality. At the plant input,

$$\bar{A}=\begin{bmatrix}\phi & 0\\ b_d C_1 H_C & A_d\end{bmatrix},\quad \bar{B}=\begin{bmatrix}\psi B_c\\ 0\end{bmatrix},\quad \bar{C}=-C_2[F_d C_1 H_C | H_d] \tag{19}$$

At the plant output,

$$\bar{A}=\begin{bmatrix}\phi & \psi B_c C_2 H_d\\ 0 & A_d\end{bmatrix},\quad \bar{B}=\begin{bmatrix}\psi B_c C_2 F_d\\ B_d\end{bmatrix},\quad \bar{C}=-C_1[H_c|0] \tag{20}$$

Using the equations from Refs. 1 and 6 in conjunction with Eq. (8), σ-gradients can be found for elements or combinations of elements of the A_d, B_d, H_d, F_d, and H_c matrices. But gradients with respect to the A_c and B_c matrices, and linear combinations thereof, have not been derived in previous documents. These gradients are of primary interest to an aircraft control system sensitivity study, because they contain all continuous-system dynamics, including aerodynamics and control power derivatives, servo dynamics, and continuous sensors and filters.

To determine gradients with respect to elements of A_c and B_c, we first apply the basic equation from Mukhopadhyay and Newsom,[6] which is valid for any parameter p:

$$\frac{\partial\sigma_n(I+KG)}{\partial p}=\mathrm{Re}\cdot\mathrm{tr}\left[\left(\bar{C}\Omega\frac{\partial\bar{A}}{\partial p}\Omega\bar{B}+\bar{C}\Omega\frac{\partial\bar{B}}{\partial p}+\frac{\partial\bar{C}}{\partial p}\Omega\bar{B}\right)v_n u_n^*\right] \tag{21}$$

where $\Omega=(Iz-\bar{A})^{-1}$, $z=e^{-sT}$, and v_n, u_n are the nth right and left normalized singular vectors of $I+KG$, respectively.

If $p=a_c$ (i.e., it is an element *of* A_c), then the derivatives $\partial\bar{A}/\partial p$, $\partial\bar{B}/\partial p$, and $\partial\bar{C}/\partial p$ that appear in Eq. (21) take on the following forms:

Input case [$L_i \neq I$; see Eq. (19)]:

$$\frac{\partial\bar{A}}{\partial p}=\frac{\partial\bar{A}}{\partial a_c}=\begin{bmatrix}\frac{1}{2}\psi\left(\frac{\partial A_c}{\partial a_c}\right)(\phi+I) & 0\\ 0 & 0\end{bmatrix} \tag{22a}$$

$$\frac{\partial\bar{B}}{\partial p}=\frac{\partial\bar{B}}{\partial a_c}=\begin{bmatrix}\frac{1}{2}\psi\left(\frac{\partial A_c}{\partial a_c}\right)\psi B_c\\ 0\end{bmatrix} \tag{22b}$$

$$\frac{\partial\bar{C}}{\partial p}=\frac{\partial\bar{C}}{\partial a_c}=0 \tag{22c}$$

Output case [$L_o \neq I$; see Eq. (20)]:

$$\frac{\partial\bar{A}}{\partial p}=\frac{\partial\bar{A}}{\partial a_c}=\begin{bmatrix}\frac{1}{2}\psi\left(\frac{\partial A_c}{\partial a_c}\right)(\phi+I) & \frac{1}{2}\psi\left(\frac{\partial A_c}{\partial a_c}\right)\psi B_c C_2 H_d\\ 0 & 0\end{bmatrix} \tag{23a}$$

$$\frac{\partial\bar{B}}{\partial p}=\frac{\partial\bar{B}}{\partial a_c}=\begin{bmatrix}\frac{1}{2}\psi\left(\frac{\partial A_c}{\partial a_c}\right)\psi B_c C_2 F_d\\ 0\end{bmatrix} \tag{23b}$$

$$\frac{\partial\bar{C}}{\partial p}=\frac{\partial\bar{C}}{\partial a_c}=0 \tag{23c}$$

where approximations to $\partial\phi/\partial a_c$ and $\partial\psi/\partial a_c$ from Ref. 11 have been used. These approximations are exact to order T^2.

Since it is apparent from Eqs. (22) and (23) that the input case results will be a subset of the output case results, we will continue for the more general output case only. The resulting formulation will apply to either case. Substituting the matrices of Eq. (22) into Eq. (21) and partitioning the other matrices appropriately yields

$$\frac{\partial\sigma_n(I+KG)}{\partial a_c}=\mathrm{Re}\cdot\mathrm{tr}\left(\frac{1}{2}\left\{\left[(\bar{C}\Omega)_1\psi\left(\frac{\partial A_c}{\partial a_c}\right)(\phi+I)\times(\bar{C}\Omega)_1\psi\left(\frac{\partial A_c}{\partial a_c}\right)\psi B_c C_2 H_d\right]\begin{pmatrix}(\Omega\bar{B})_1\\(\Omega\bar{B})_2\end{pmatrix}+(\bar{C}\Omega)_1\psi\left(\frac{\partial A_c}{\partial a_c}\right)\psi B_c C_2 F_d\right\}v_n u_n^*\right) \tag{24}$$

where $(\bar{C}\Omega)_1$ represents the left-hand quadrant of the $\bar{C}\Omega$ matrix

$$\bar{C}\Omega = [(\bar{C}\Omega)_1 \quad (\bar{C}\Omega)_2] \tag{25}$$

and $\Omega\bar{B}$ is partitioned vertically, as shown in Eq. (24). Using the matrix operation[12]

$$\frac{\partial}{\partial x}[\mathrm{tr}\{yxz\}] = y^*z^* \tag{26}$$

and the matrix trace property

$$\mathrm{Re}\cdot\mathrm{tr}(A) = \mathrm{Re}\cdot\mathrm{tr}(A^*)$$

this formula can be written as a matrix relation for all of the elements of A_c as

$$\frac{\partial\sigma_n(I+KG)}{\partial A_c^T} = \mathrm{Re}\{\tfrac{1}{2}[(\phi+I)(\Omega\bar{B})_1 v_n u_n^*(\bar{C}\Omega)_1 + \psi B_c C_2 H_d(\Omega\bar{B})_2 v_n u_n^*(\bar{C}\Omega)_1 + \psi B_c C_2 F_d v_n u_n^*(\bar{C}\Omega)_1]\psi\} \tag{27}$$

Equation (27) can be greatly simplified by recognizing the following matrices as partitions of previously derived terms [see Refs. 1 and 2 and Eq. (20)]:

$$(\Omega\bar{B})_1 v_n u_n^*(\bar{C}\Omega)_1 = \left(\frac{\partial\sigma_n(I+KG)}{\partial\bar{A}^T}\right)_{11} \tag{28a}$$

$$\psi B_c C_2 H_d = (\bar{A})_{12} \tag{28b}$$

$$(\Omega\bar{B})_2 v_n u_n^*(\bar{C}\Omega)_1 = \left(\frac{\partial\sigma_n(I+KG)}{\partial\bar{A}^T}\right)_{21} \tag{29a}$$

$$\psi B_c C_2 F_d = (\bar{B})_1 \tag{29b}$$

and

$$v_n u_n^*(\bar{C}\Omega)_1 = \left(\frac{\partial\sigma_n(I+KG)}{\partial\bar{B}^T}\right)_1 \tag{30}$$

where $\bar{B}$ and $\partial\sigma_n/\partial\bar{B}^T$ have been partitioned vertically, and $\bar{A}$ and $\partial\sigma_n/\partial\bar{A}^T$ have been partitioned into four quadrants [partitioned matrix dimensions correspond to the partitioning in Eq. (20)]. The final equation, then, for derivatives with respect to A_c is

$$\frac{\partial\sigma_n(I+KG)}{\partial A_c^T} = \mathrm{Re}\left\{\frac{1}{2}\left[(\phi+I)\left(\frac{\partial\sigma_n}{\partial\bar{A}^T}\right)_{11} + \bar{A}_{12}\left(\frac{\partial\sigma_n}{\partial\bar{A}^T}\right)_{21} + \bar{B}_1\left(\frac{\partial\sigma_n}{\partial\bar{B}^T}\right)_1\right]\psi\right\} \tag{31}$$

For the case where the disturbance is at the input, a derivation similar to that given above can be done.[13] Doing so verifies that Eq. (31) is valid for the input case also, even though $\bar{A}$, $\bar{B}$, and $\bar{C}$ are different. For gradients with respect to B_c matrix elements, different equations are obtained at the input and at the output. These equations are:

Input case:

$$\frac{\partial\sigma_n(I+KG)}{\partial B_c^T} = \left(\frac{\partial\sigma_n}{\partial\bar{B}^T}\right)_1\psi \tag{32}$$

Output case:

$$\frac{\partial\sigma_n(I+KG)}{\partial B_c^T} = C_2\left[F_d\left(\frac{\partial\sigma_n}{\partial\bar{B}^T}\right)_1 + H_d\left(\frac{\partial\sigma_n}{\partial\bar{A}^T}\right)_{21}\right]\psi \tag{33}$$

Demonstration of the Singular-Value Sensitivity Analysis on the X-29A Advanced Technology Demonstrator

The X-29A lateral-directional primary flight control system represents a good example of a high-order, digital, multiloop, control system. A simplified block diagram of the feedback portion of the control system is shown in Fig. 3. This is the linearized version of the control laws, for the "normal digital, up and away" mode only. Feedforward and command-shaping dynamics have not been included in Fig. 3 because they do not affect this type of stability analysis.

Because singular values are a relatively new tool for judging aircraft relative stability, rules of thumb such as "10 dB gain margin, 45 deg phase margin" have not yet been developed. Thus, it is of interest to tabulate some singular-value results for an airplane that is currently flying. Table 1 gives the minimum of the return-difference-matrix $\underline{\sigma}$-plot for several flight conditions at which the X-29A has already flown. D-matrix scaling (as described in the first section) has been performed on these systems, so that the values in Table 1 are equivalent to those that would be obtained using "structured" singular values[9,10] with disturbances that are assumed to have no frequency shaping. Single-loop frequency response results are also given in Table 1 for comparison. Since the X-29A exhibits acceptable stability properties at these flight conditions, it can be deduced that a minimum singular value of 0.5 is reasonable for a well-developed, accurate model of the system. This conclusion is, of course, based on limited experience—more data such as that shown in Table 1 must be compiled.

Combining the singular-value gradients developed here and in Refs. 1 and 2 with the D-matrix scaled $\underline{\sigma}$-plots and additional engineering data, it is possible to define a sensitivity analysis that will help the control designer judge if the vehicle model is adequate (i.e., expected model variations will not have a significant impact on the system performance) or what further model refinements are required. Note that this is not a robustness analysis but a method for identifying the accuracy needed in a plant model, and the specific parameters that must be accurately known. The steps in the procedure are illustrated

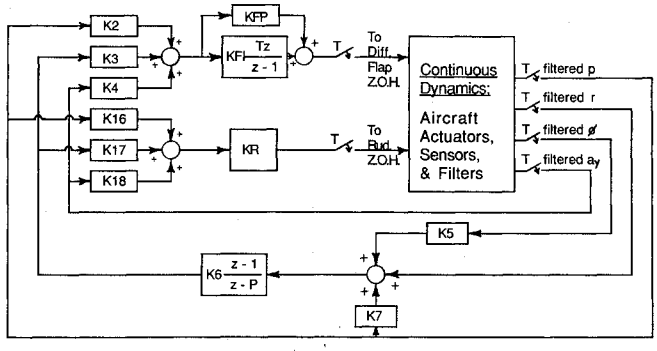

Fig. 3 X-29A lateral-directional normal mode control laws (feedforward dynamics have been omitted).

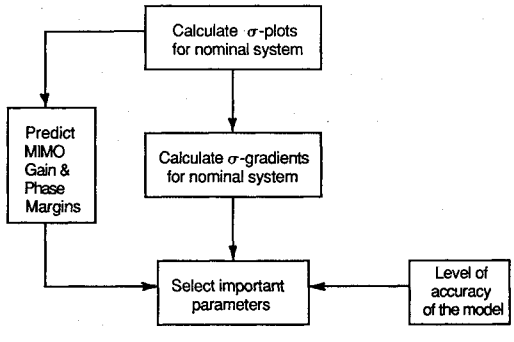

Fig. 4 Sensitivity analysis procedure.

Table 1 Comparison of single-loop and multiloop stability analysis results for the X-29A

	Lateral (SISO)		Directional (SISO)		Singular value (MIMO)	
Flight condition	Gain margin	Phase margin	Gain margin	Phase margin	Input node σ	Output node $\underline{\sigma}$
$M = 0.30$, H = 15,000 ft	15.6 dB at 17.9 rad/s	70 deg at 3.7 rad/s	15.9 dB at 8.9 rad/s	70 deg at 2.8 rad/s	0.65 at 5.0 rad/s	0.58 at 4.6 rad/s
$M = 0.40$, H = 15,000 ft	16.3 dB at 17.3 rad/s	70 deg at 3.6 rad/s	12.5 dB at 9.6 rad/s	56 deg at 3.7 rad/s	0.56 at 5.7 rad/s	0.49 at 5.3 rad/s
$M = 0.40$, H = 30,000 ft	15.9 dB at 18.2 rad/s	68 deg at 3.6 rad/s	15.0 dB at 8.8 rad/s	65 deg at 2.9 rad/s	0.63 at 5.0 rad/s	0.54 at 4.3 rad/s
$M = 0.60$, H = 15,000 ft	14.1 dB at 14.5 rad/s	72 deg at 3.7 rad/s	15.1 dB at 12.3 rad/s	67 deg at 4.4 rad/s	0.61 at 7.1 rad/s	0.62 at 7.0 rad/s
$M = 0.60$, H = 30,000 ft	16.3 dB at 16.7 rad/s	73 deg at 3.4 rad/s	17.9 dB at 12.5 rad/s	75 deg at 3.4 rad/s	0.71 at 6.6 rad/s	0.69 at 6.5 rad/s
$M = 0.70$, H = 30,000 ft	17.5 dB at 15.5 rad/s	75 deg at 2.6 rad/s	12.9 dB at 13.0 rad/s	64 deg at 4.6 rad/s	0.67 at 7.9 rad/s	0.66 at 8.0 rad/s
$M = 0.90$, H = 30,000 ft	19.3 dB at 14.2 rad/s	71 deg at 2.3 rad/s	8.9 dB at 13.3 rad/s	49 deg at 6.8 rad/s	0.54 at 9.8 rad/s	0.54 at 9.8 rad/s

in Fig. 4. This procedure must be performed at both the input and the output of the plant.

The first step is to find the scaling matrix D, as discussed earlier, and to plot the singular values of the unperturbed control system. From the σ-plot the designer can judge the relative stability of the nominal design. Next, $\underline{\sigma}$-gradient plots can be done for all parameters of the control system that are of interest. To judge whether a parameter is important or not, the percent variation required to drive the system to an unacceptable level of stability (designated σ_{ma}) is computed for each p, using

$$\Delta p \cong \min_{\omega} \left\{ \frac{\sigma(\omega) - \sigma_{ma}}{\left(\frac{\partial \sigma}{\partial p}(\omega) \right)} \right\} \tag{34}$$

Good judgment and experience with singular values must be applied to choose σ_{ma}. The size of Δp for each parameter (plus information gained by studying the σ-plots and σ-gradient plots themselves) can be combined with data about the estimated accuracy of each system parameter to determine the set of parameters that dominate the relative stability of the control system.

Several words of caution should be noted. Firstly, although the calculation of the singular-value gradients produces useful information, the control designer must have a thorough understanding of his system to correctly interpret the results. Parameters must be chosen with care so that their variations are mutually independent and physically realizable. Secondly, since these are first-order gradients and, in general, the singular values do not vary linearly with parameter variations, caution should be exercised when predictions based on Eq. (34) require large changes in the singular values. Because the purpose of the sensitivity analysis is to give a list of candidate parameters for further study, nonlinearities do not conflict with the basic intent of the analysis. The range of accuracy of the linearity assumption is studied below. Finally, gradients with respect to other singular values of the system besides the minimum singular value may also be important. For instance, if a parameter variation causes a singular value that is not the minimum to become the minimum, then that parameter is potentially an important one, depending on the magnitude of the parameter variation required to do so.

To demonstrate the technique, the X-29A lateral-directional control laws were analyzed in straight and level flight at a Mach number of 0.9 and an altitude of 30,000 ft. D-matrix scaling was performed, the σ-plots were computed, and gradients were taken. Then, Eq. (34) was applied. The results appear in Table 2 for all the important elements of the aircraft aerodynamic and control power matrices. Gradients with respect to continuous-system parameters required the use of Eqs. (8) and (27). Gradients were performed at both the input and the output of the continuous plant, for both the minimum and the next-to-smallest singular values. The gradients that had the greatest effect were then concatenated into Table 2. In all cases it was discovered that, although slight differences existed between input and output gradients, studying the gradients for the minimum singular values of the input return-difference matrix above would have yielded adequate results.

Table 2 Sensitivity of the X-29 to changes in lateral system parameters. Parameters are in descending order of importance ($M = 0.9$, H = 30,000 ft)

Parameter variations necessary to drive $\sigma_{\min}$ to 0.30 in the critical frequency range: 2.0 to 100 rad/s					
Param. (p)	$\omega_{\min}$	$\sigma(\omega_{\min})$	$\partial\sigma/(\partial p/p)$	Δp, %	$\Delta\sigma$, %
Aero derivatives:					
$B(3,2) - N'_{\delta r}$	10.5	0.544	0.332	−74	−45[a]
$B(2,1) - L'_{\delta a}$	2.04	1.16	0.433	−199	−74
$A(2,2) - L'_{p}$	2.03	0.672	−0.148	251	−55[a]
$B(2,2) - L'_{\delta r}$	11.2	0.563	−0.077	343	−47[a]
$B(3,1) - N'_{\delta a}$	7.23	0.844	−0.113	480	−64[b]
$A(1,2) - Y'_{p}$	5.40	1.26	0.109	−880	−76[b]
$A(3,1) - N'_{\beta}$	9.77	0.536	−0.026	919	−44[a]
$A(2,1) - L'_{\beta}$	2.03	0.672	−0.036	1039	−55[a]
$A(3,2) - N'_{p}$	8.52	0.559	0.024	−1087	−46[a]
$A(2,3) - L'_{r}$	7.97	0.610	0.005	—	−51
$A(1,2) - Y'_{\delta r}$	7.97	0.610	0.005	—	−51
$A(3,3) - N'_{r}$	7.23	0.689	−0.005	—	−56
$A(1,1) - Y'_{\beta}$	7.23	0.689	−0.003	—	−56
$B(1,1) - Y'_{\delta a}$	6.56	0.768	−0.002	—	−61

Definitions:
Param. = parameter for which gradient has been taken
$\omega_{\min}$ = frequency at which this parameter has maximum effect
$\sigma(\omega_{\min})$ = singular value at $\omega_{\min}$
$\partial\sigma/(\partial p/p)$ = normalized singular-value gradient at $\omega_{\min}$
Δp = percentage change in p necessary to drive $\sigma_{\min}$ to 0.30
$\Delta\sigma$ = percentage change in σ necessary at $\omega_{\min}$ to get to 0.30

[a]Results are from gradients of output minimum singular values.
[b]Results are from gradients of next-to-smallest input singular values.

Table 2 can be used to determine which system parameters in the X-29A should be studied further. The last two columns of Table 2 are the most revealing. Column 4 is used to order the

parameters from most to least important; it indicates the percent variation in the parameter required to drive the minimum of the σ-plot to a σ_{ma} of 0.3 [using Eq. (34)]. Looking at this column, it is apparent that the X-29A is quite insensitive to most aerodynamic parameter variations. The most important aerodynamic parameter N_{δ_r} must decrease by 74% in order to drive the system to an unacceptable level of relative stability. Combinations of aerodynamic variations could also be included in this type of table, using Eq. (8).

To demonstrate the way that a parameter variation effects the σ-plot, Fig. 5 shows the σ-plot for the unperturbed X-29A at $M = 0.9$ and $H = 30{,}000$ ft, together with the σ-plot for the system after a 100% variation in N_{δ_r}. The N_{δ_r} σ-gradient is also included in this plot to show how the gradient predicts the changes in the σ-plot. Careful study of Fig. 5 reveals that the actual changes caused by varying N_{δ_r} are not predicted exactly by the σ-gradient plot. Differences occur because the σ-plot is not a linear function of N_{δ_r}, i.e., the assumption that

$$\Delta\sigma \cong \frac{\partial\sigma}{\partial p} \cdot \Delta p \tag{35}$$

is not exact. It has been found that the validity of the linearity assumption of Eq. (35) is a strong function of $\Delta\sigma$, the predicted percent change in σ due to Δp. Because $\Delta\sigma$ is so important to the accuracy of the predictions of column 4 in Table 2, it is included as column 5.

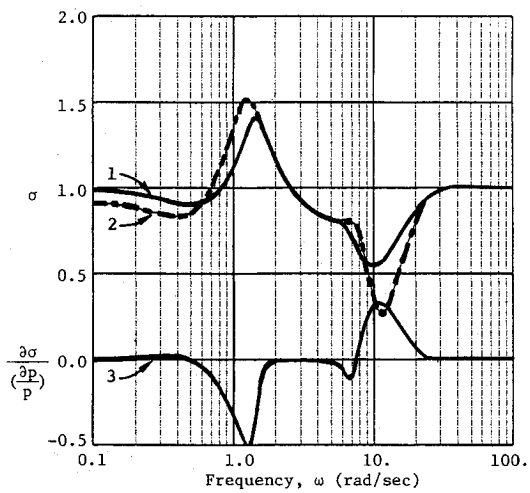

Fig. 5 σ-plot for the X-29A at $M = 0.9$, $H = 30{,}000$ ft before (1) and after (2) a 100% variation in the parameter $N_{\delta r}$, whose gradient is also included (3).

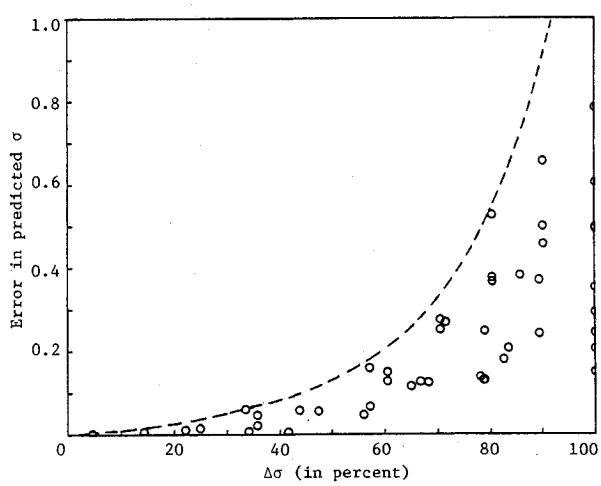

Fig. 6 Error between predicted and actual σ, as a function of the predicted percentage change in σ.

To find out the range of $\Delta\sigma$ for which the gradient predictions are good, perturbations similar to that shown in Fig. 5 were conducted for many parameters in the X-29A lateral-directional control system. The results are summarized in Fig. 6. The independent variable in this plot is $\Delta\sigma$, whereas the dependent variable is the error between the predicted and actual minimum of the σ-plot after a single parameter variation. This choice of variables was found to give the highest degree of correlation. The most important parameters (those whose gradients were highest) were varied, one by one, to give each of the data points in Fig. 6. The resulting "envelope" indicates that changes in the σ-plot of up to about 45% can be predicted within the accuracy necessary for a sensitivity analysis.

Conclusions

The singular-value sensitivity analysis technique can be extended to encompass commonly encountered systems. Tabular and graphical sensitivity data showing the effect of single parameters or linear combinations of parameters on relative stability can be computed for high-order, digital, multiloop control systems. The results are of a first-order nature, due to linearity assumptions and approximations made during the development.

Appendix: Data for the X-29 Lateral-Directional Control System at $M = 0.9$, $H = 30{,}000$ ft

Figure 3 shows a block diagram of a linear sampled-data representation of the X-29 lateral-directional flight control system (feedback dynamics only). The numerical data for this block diagram at $M = 0.9$, and 30,000 ft are given in this Appendix. The continuous dynamics will be given in three parts: the basic aircraft, the actuators, and the sensors and filters.

The basic aircraft dynamics can be represented by a simple perturbed-state matrix differential equation:

$$\dot{x} = \begin{bmatrix} -0.1645 & 0.06490 & -0.9979 & 0.03575 \\ -24.13 & -2.506 & 1.075 & 0.0 \\ 6.654 & -0.09662 & -0.04137 & 0.0 \\ 0.0 & 1.0 & 0.06504 & 0.0 \end{bmatrix} x + \begin{bmatrix} -0.0008210 & 0.0006588 \\ 1.143 & 0.2883 \\ 0.07125 & -0.07290 \\ 0.0 & 0.0 \end{bmatrix} \delta$$

where the four perturbed states in x are sideslip angle β, roll rate p, yaw rate r, and bank angle ϕ (in radians and radians/s), and the two controls are differential flap and rudder (in degrees).

The actuator dynamics for the rudder and the differential flaps are modeled as transfer functions with identical characteristics. The transfer function used for both the differential flap servo and the rudder servo is

$$\frac{\delta_{\text{out}}(s)}{\delta_{\text{in}}(s)} = \left(\frac{2928}{s^2 + 165.1s + 2928}\right)\left(\frac{5098}{s^2 + 105s + 5098}\right)\left(\frac{100}{s + 100}\right)$$

The shaping and anti-aliasing filters for the continuous states that the controller requires (p, r, δ, and side acceleration a_y) are combined into the transfer functions below, where the subscript f denotes the filtered quantities that go into the samplers in Fig. 3.

$$\frac{p_f(s)}{p(s)} = \left(\frac{24{,}650}{s^2 + 220s + 24{,}650}\right)\left(\frac{200}{s + 200}\right)$$

$$\frac{r_f(s)}{r(s)} = \left(\frac{18{,}770}{s^2 + 193s + 18{,}770}\right)\left(\frac{s^2 + 14s + 4900}{s^2 + 98s + 4900}\right)\left(\frac{200}{s + 200}\right)$$

$$\frac{\phi_f(s)}{\phi(s)} = \left(\frac{30}{s + 30}\right)$$

$$\frac{a_{y_f}(s)}{a_y(s)} = \left(\frac{s^2 + 13.6s + 4624}{s^2 + 68s + 4624}\right)\left(\frac{200}{s + 200}\right)$$

To complete the description of the control system, the gains and parameters in the block diagram in Fig. 3 are

$K2 = -1.0$	$KFP = 0.028$	$P = 0.9876$
$K3 = 3.0$	$KFI = 0.0812$	$T = 0.025$
$K4 = 0.0$	$KR = 1.0$	
$K5 = -0.03596$	$K16 = 0.0$	
$K6 = 0.9938$	$K17 = 1.102$	
$K7 = -0.0649$	$K18 = 0.0$	

Acknowledgments

This work was sponsored by the NASA Ames Research Center, Dryden Flight Facility, under Cooperative Agreement NCC 2-293.

References

[1]Herrera-Vaillard, A., Paduano, J. D., and Downing, D. R., "Sensitivity Analysis of Automatic Flight Control Systems Using Singular Value Concepts," AIAA Paper 85-1899, Aug. 1985.

[2]Herrera-Vaillard, A., Paduano, J. D., and Downing, D. R., "Development of a Sensitivity Analysis Technique for Multiloop Flight Control Systems," NASA CR-166619, Oct. 1985.

[3]Ly, U., "Robustness Analysis of a Multiloop Flight Control System," AIAA Paper 83-2189, Aug. 1983.

[4]Yeh, H. H., Ridgely, Capt. B., and Banda, S. S., "Nonconservative Evaluation of Uniform Stability Margins of Multivariable Feedback Systems," AIAA Paper 84-1939, Aug. 1984.

[5]Mukhopadhyay, V. and Newsom, J. R., "Application of Matrix Singular Value Properties for Evaluating Gain and Phase Margins of Multiloop Systems," AIAA Paper 83-1574, Aug. 1982.

[6]Newsom, J. R. and Mukhopadhyay, V., "The Use of Singular Value Gradients and Optimization Techniques to Design Robust Controllers for Multiloop Systems," AIAA Paper 83-2191, Aug. 1983.

[7]Anderson, L. R., "Direct Design of Multivariable Control Systems through Singular Value Decomposition," AIAA Paper 83-2276, Aug. 1983.

[8]Lehtomaki, N. A., Sandell, N. R., Jr., and Athans, M., "Robustness Results in Linear-Quadratic Gaussian Based Multivariable Control Designs," *IEEE Transactions on Automatic Control*, Vol. AC-26, Feb. 1981, pp. 75–92.

[9]Thompson, Peter. "Note on Multivariable Gain and Phase Margins," California Inst. of Technology, Pasadena, CA, March 1986.

[10]Doyle, J. C., Wall, J. E., and Stein, G., "Performance and Robustness Analysis for Structured Uncertainties," *Proceedings of the 21st IEEE Conference on Decision and Control*, Vol. 2, Inst. of Electrical and Electronic Engineers, New York, 1982, pp. 629-636.

[11]Maine, R. E. and Iliff, K. W., "Formulation and Implementation of a Practical Algorithm for Parameter Estimation with Process and Measurement Noise," *SIAM Journal of Applied Mathematics*, Vol. 41, No. 3, Dec. 1981, pp. 558-579.

[12]*Applied Optimal Estimation*, Tech. Staff, Analytic Sciences Corp., edited by Arthur Gelb, MIT Press, Cambridge, MA, 1974.

[13]Paduano, J. D., "Application of a Sensitivity Analysis Technique to High-Order Digital Flight Control Systems," NASA CR-179429, Sept. 1987.